

## Applications of recently proposed closure approximations to injection molding filling simulation of short-fiber reinforced plastics

Du Hwan Chung and Tai Hun Kwon\*

Department of Mechanical Engineering, Pohang University of Science and Technology,  
San 31 Hyojadong Nam-ku, Pohang, Kyungbuk, 790-784, Korea

(Received May 17, 2000; final revision received October 20, 2000)

### Abstract

The present work is aimed at performing injection molding filling simulation of fiber suspension in polymer based matrix. The numerical simulation incorporates the coupling effect between the flow field and the fiber orientation state together with in-plane velocity gradient effect with recently proposed closure approximations. Predicted orientation components are compared with available experimental data of a film-gated strip and a center-gated disk. Predictions with IBOF closure approximation show excellent behaviors with regard to accuracy and numerical efficiency. However, predicted results seem to have consistent errors in comparison with experimental data. Diffusivity term which accounts for fiber-fiber interaction might have to be modified.

### 1. Introduction

Nowadays, injection/compression molded plastic parts with reinforced particles become more and more important due to its light weight, cost effectiveness, ease of manufacturing, etc., Fiber suspension in polymer based matrix is one of the kind and in this work, non-Brownian short fibers are considered. Fiber reinforced composite typically shows anisotropic mechanical, thermal and rheological properties. Prediction of thermo-mechanical properties with given fiber orientation has been well developed to some extent [Halpin and Kardos (1976)]. Therefore, prediction of fiber orientation during the transient mold filling is important for the prediction of such anisotropic properties of final plastic part.

Nowadays, many researchers have developed many numerical simulation programs with different methods. However, some of them using direct calculation of fiber motion [Yamamoto and Matsuoka (1993), Yamane *et al.* (1994), Mackaplow and Shaqfeh (1996), Sundararajakumar and Koch (1997), Fan *et al.* (1998)] require incredible computation time which is the reason why such a numerical simulation method cannot be accommodated. Calculation of fiber orientation state using the probability distribution function (DFC, in short) is one of them. Instead, a tensor representation of orientation state [Advani and Tucker (1987)], which is a pre-aver-

aging concept of DFC, is widely used for its efficiency, compactness and above all, manageable computation time. However, it is necessary to introduce a closure approximation to express the higher order tensor in terms of lower order tensors for a closed set of equation since the evolution equation for orientation tensor involves the next higher even order tensor.

Various closure approximations have been proposed. Among them, a Hybrid closure approximation (HYB) [Advani and Tucker (1990)] has readily been used for its stable behaviors in spite of its over-prediction of orientation components compared with DFC. Recently, Cintra and Tucker (1995) developed Orthotropic fitted closure approximation (ORF, ORL) by assuming that the principal directions of 4<sup>th</sup> order orientation tensor are functions of the eigenvalues of 2<sup>nd</sup> order orientation tensor. Unknown parameters were determined by fitting selected flow data obtained from DFC. ORF (or ORL) shows better behaviors than previous closure approximations but unfortunately suffers from non-physical oscillations at low value of fiber-fiber interaction coefficient. Chung and Kwon have proposed ORW and ORW3 (1999, 2000a) which overcome such problems of non-physical oscillations. However, such Orthotropic type closure approximations (ORF, ORL, ORW and ORW3) requires additional computation time for the transformation between the global coordinate system and the principal coordinate system. In this respect, Chung and Kwon (2000b) have proposed IBOF (Invariant Based Optimal Fitting) closure approximation which significantly reduces the computation time.

\*Corresponding author: thkwon@postech.ac.kr  
© 2000 by The Korean Society of Rheology

For proper numerical simulation, coupling effect between the flow field and fiber orientation state must be incorporated. Chung and Kwon (1995,1996) implemented the Dinh-Armstrong model [Dinh and Armstrong (1984)] incorporating the additional stress due to the existence of fibers into the governing equation based on the Hele-Shaw approximation in injection molding filling simulation of short-fiber reinforced plastic parts. Present work is aimed at injection molding filling simulations incorporating the coupling effect between the flow and fiber orientation along with the in-plane velocity gradient effect with recently developed closure approximations. Predicted values will be compared with available experimental data of a film-gated strip and a center-gated disk from Bay (1991).

## 2. Theory

### 2.1. Fiber Orientation

There are several different approaches describing the fiber orientation state in short-fiber-reinforced part during molding process, but among other things orientation tensors are mainly used for a compact representation of the orientation state of fibers because of the computational efficiency.

Fiber is considered to be rigid cylinder and its aspect ratio is assumed to be mono-disperse. Single fiber can be represented as a unit vector  $\mathbf{p}$  (or  $\theta$ , the polar angle, and  $\phi$ , the azimuthal angle) as shown in Fig. 1. The orientation state of a group of fibers can be described by a probability distribution function  $\Psi(\mathbf{p})$ , defined so that the probability of a fiber being oriented within an angular range  $d\mathbf{p}$  of the direction  $\mathbf{p}$  is equal to  $\Psi(\mathbf{p})d\mathbf{p}$ . Combining the following conservation equation, Eq.1, for  $\Psi$

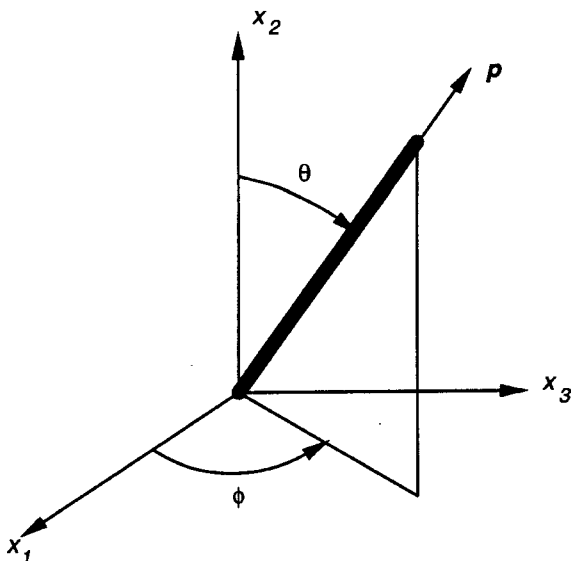


Fig. 1. Orientation of single fiber.

in  $\mathbf{p}$  space and the fiber angular velocity equation, Eq.2, leads to the governing equation for  $\Psi(\mathbf{p})$  [Folgar and Tucker (1984), Advani and Tucker (1987)].

$$\frac{D\Psi}{Dt} = \frac{\partial}{\partial \mathbf{p}} \cdot (\Psi \dot{\mathbf{p}}) \quad (1)$$

$$\dot{p}_i = -\frac{1}{2}\omega_{ij}p_j + \frac{1}{2}\lambda(\dot{\gamma}_{ij}p_j - \dot{\gamma}_{ki}p_k p_i p_i) - \frac{D_r \partial \Psi}{\Psi \partial p_i} \quad (2)$$

Direct calculation of probability distribution function  $\Psi(\mathbf{p})$  is referred to as 'DFC'.

The second and fourth order orientation tensors are defined as follows:

$$\begin{aligned} a_{ij} &= \int p_i p_j \Psi(\mathbf{p}) d\mathbf{p} \\ a_{ijkl} &= \int p_i p_j p_k p_l \Psi(\mathbf{p}) d\mathbf{p} \end{aligned} \quad (3)$$

The evolution equation for the second-order orientation tensor  $a_{ij}$  can be expressed as follows [Advent and Tucker (1987)] :

$$\begin{aligned} \frac{Da_{ij}}{Dt} &= -\frac{1}{2}(\omega_{ik}a_{kj} - a_{ik}\omega_{kj}) + \frac{1}{2}\lambda(\dot{\gamma}_{ik}a_{kj} + a_{ik}\dot{\gamma}_{kj} - 2\dot{\gamma}_{kl}a_{ijkl}) \\ &+ 2D_r(\delta_{ij} - 3a_{ij}) \end{aligned} \quad (4)$$

where  $\omega_{ij} = u_{j,i} - u_{i,j}$  is the rotation rate tensor,  $\dot{\gamma}_{ij} = u_{j,i} + u_{i,j}$  the rate of deformation tensor, and  $\delta_{ij}$  the identity tensor.  $\lambda = \frac{(L/D)^2 - 1}{(L/D)^2 + 1}$  is a parameter related to the aspect ratio of the fiber  $L/D$ . The third term on the right hand side of Eq.4 accounts for fiber-fiber interaction. The rotary diffusivity term  $D_r$  is used to model fiber-fiber interaction in concentrated (semi-dilute) suspensions. Folgar and Tucker (1984) suggested  $D_r = C_1 \dot{\gamma}$ , where an interaction coefficient  $C_1$  should be determined, to our present knowledge, in such a way that the predicted orientation can fit best the experimental data,  $\dot{\gamma}$  being the generalized shear rate defined as follows

$$\dot{\gamma} = \sqrt{\frac{1}{2} \dot{\gamma}_{ij} \dot{\gamma}_{ji}} \quad (5)$$

The present study adopted  $D_r = C_1 \dot{\gamma}$  in the numerical calculations of fiber orientation.

### 2.2. Closure Approximations

A closure approximation is inherently required to obtain a closed set of evolution equations for orientation tensors: for instance, to solve Eq. 4 one needs to introduce a suitable closure approximation for the fourth-order tensor  $a_{ijkl}$  in terms of  $a_{ij}$  and  $\delta_{ij}$ .

The present study employed several closure approximations which can be briefly described below.

#### Orthotropic fitted closure approximation (ORF, ORL)

Cintra and Tucker (1995) have developed Orthotropic fitted closure approximations (referred to as ORF, ORL)

by assuming the principal values of  $a_{ijkl}$  are functions of the eigenvalues of  $a_{ij}$ . Short summary might be presented as follows:

With full symmetry conditions and normalization conditions, there are only three independent components of principal values of 4<sup>th</sup> order tensor, which are taken to be functions of two largest eigenvalues of 2<sup>nd</sup> order tensor  $a_{ij}$  as follows :

$$\begin{aligned} \bar{A}_{11} &= f_{11}(a_1, a_2) \\ \bar{A}_{22} &= f_{22}(a_1, a_2) \\ \bar{A}_{33} &= f_{33}(a_1, a_2) \end{aligned} \quad (6)$$

where  $\bar{A}_{11}, \bar{A}_{22}, \bar{A}_{33}$  are independent principal values of 4<sup>th</sup> order orientation tensor in contracted notation ( $A_{11} = a_{1111}^p, A_{22} = a_{2222}^p, A_{33} = a_{3333}^p, A_{44} = a_{1122}^p, A_{55} = a_{2233}^p, A_{66} = a_{3311}^p$ ) and  $a_1, a_2$  are two largest eigenvalues of 2<sup>nd</sup> order orientation tensor, that is,  $a_1 \geq a_2 \geq a_3$ . To determine unknown parameters in Eq.6 least square optimal fitting were used with selected flow cases generated by DFC.

Even if ORF and ORL satisfactorily predict most simple flows, one of the critical problems of ORF and ORL is that they suffer from non-physical oscillations in simple shear flow for low  $C_1$  values.

**ORW and ORW3**

ORW and ORW3 [Chung and Kwon (1999, 2000a)] were proposed as an improved version of ORF and ORL closure approximations to overcome non-physical oscillations observed in ORF and ORL. The main improvement was achieved by fitting additional flow data to cover the whole region of fiber orientation states. ORW3 outperforms ORW especially for non-homogeneous radial diverging flow for low  $C_1$  values.

**Natural closure approximation (NAT)**

NAT takes a general expression for  $a_{ijkl}$  in terms of  $a_{ij}$  and  $\delta_{ij}$  and polynomial expansions in terms of principal invariants were adopted for unknown coefficients appearing in the general expression. The term ‘‘Natural’’ closure approximation is originated from the fact that it made use of the natural closure values, i.e., analytical solutions which exist only for  $C_1 = 0.0$  with  $\lambda = 1$  in a least square fitting procedure [Verleye and Dupret (1994)]. It showed good transient behaviors but results in a little over-prediction of steady state orientations. It may be noted, however, that singularities are reported to exist for axisymmetric orientation states, which is referred to as a significant drawback of using NAT in general flow cases without a special care of such singularities [Dupret and Verleye (1999)].

**ORE**

Recently, Wetzel (1999) and Verweyst (1999) introduced another version of Orthotropic fitted closure approximation, ORE, differing from ORF (or ORL) in that analytic solutions corresponding to  $C_1 = 0$  and  $\lambda = 1$

were adopted for the fitting flow data, as was done in NAT. It may be just mentioned that the performance of fiber orientation predictions in many flow cases is almost as good as ORW3.

**Invariant Based Optimal Fitting closure approximation (IBOF)**

IBOF [Chung and Kwon (2000b)] also starts with the most general expression of a full symmetric 4<sup>th</sup> order tensor  $a_{ijkl}$  in terms of  $a_{ij}$  and  $\delta_{ij}$  as follows :

$$\begin{aligned} a_{ijkl} &= \beta_1 \mathbf{S}(\delta_{ij} \delta_{kl}) + \beta_2 \mathbf{S}(\delta_{ij} a_{kl}) + \beta_3 \mathbf{S}(a_{ij} a_{kl}) + \beta_4 \mathbf{S}(\delta_{ij} a_{km} a_{ml}) \\ &\quad + \beta_5 \mathbf{S}(a_{ij} a_{km} a_{ml}) + \beta_6 \mathbf{S}(a_{im} a_{mj} a_{kn} a_{nl}) \end{aligned} \quad (7)$$

where the operator  $\mathbf{S}$  indicate the symmetric part of its argument, for instance,

$$\begin{aligned} \mathbf{S}(T_{ijkl}) &= \frac{1}{24} (T_{ijkl} + T_{ijkl} + T_{ijkl} + T_{ijkl} + T_{ijkl} + T_{ijkl} + T_{ijkl} + T_{ijkl} \\ &\quad + T_{ijkl} + T_{ijkl} + T_{ijkl} + T_{ijkl} + T_{ijkl} + T_{ijkl} + T_{ijkl} + T_{ijkl} + T_{ijkl} + T_{ijkl} \\ &\quad + T_{ijkl} + T_{ijkl} + T_{ijkl} + T_{ijkl} + T_{ijkl} + T_{ijkl}) \end{aligned} \quad (8)$$

IBOF assumes that the coefficients  $\beta_1 \sim \beta_6$  are polynomial expansions of the second and third invariants (II,III) of  $a_{ij}$ . It can be easily shown that, among the six  $\beta_i$ 's in Eq.7, there are only three independent values with the rest being determined in terms of the three independent ones with the help of the normalization conditions and full symmetry between indices together with Cayley-Hamilton Theorem. Orthotropic type closure approximations (ORF, ORL, ORW, ORW3) requires additional computation time for the transformation between the global coordinate and principal coordinate and most of times are spent for this procedure. IBOF does not require such computation and total CPU time is about half the computation time Orthotropic type closure approximations required.

**2.3. Mold Filling Flow**

The anisotropic constitutive equation, including an additional stress due to the existence of fibers, should be introduced for the coupled analysis of the injection molding filling of fluid flow and the fiber orientation state. Using Batchelor’s cell model [Batchelor (1971)], Dinh and Armstrong (1984) developed a rheological equation of state for semi-concentrated fiber suspensions where the average spacing  $h$  between neighboring fibers is greater than its diameter  $D$ , but less than its length  $L$  where hydrodynamic interactions between fibers dominates over mechanical contacts. The constitutive equation of this model can be described as follows:

$$\tau_{ij} = \eta(u_{i,j} + u_{j,i}) + \eta N u_{k,i} a_{ijkl} \quad (9)$$

where the dimensionless parameter  $N$  representing the

anisotropic contributions from the fibers is given by

$$N = \frac{\pi n L^3}{6 \ln(2h/D)} \quad (10)$$

with

$$h = \begin{cases} (nL^2)^{-1} & \text{for random orientation} \\ (nL)^{-1/2} & \text{for aligned orientation} \end{cases}$$

In the simulation, it is assumed that the average distance from a given fiber to its nearest neighbors  $h$  is linear in terms of the scalar measure of orientation  $f$ , which varies from zero to unity according to the orientation state of fibers. When the number of fibers per unit volume  $n$  is greater than  $1/(DL^2)$ , the average distance between fibers is assumed to be the same as for the aligned orientation state independent of the orientation state. Therefore, in this study,  $h$  is described as

$$h = (1 - f)h_{\text{random}} + fh_{\text{aligned}} \quad \text{for } \frac{\pi(D/L)^2}{4} < v_f < \frac{\pi(D/L)}{4}$$

$$h = h_{\text{aligned}} \quad \text{for } \frac{\pi(D/L)}{4} \leq v_f < \frac{\pi}{4} \quad (11)$$

$$f = 1 - 27 \det[a_{ij}] \quad (12)$$

where  $v_f$  stands for the fiber volume fraction.

The injection mold filling flow for fiber suspensions including coupling effects between flow and fiber orientation with in-plane velocity gradient effects is governed by the following equations:

**pressure equation** [Chung and Kwon (1996)]

$$\frac{\partial}{\partial x} \left[ (S - S^x) \frac{\partial P}{\partial x} - S^{xy} \frac{\partial P}{\partial y} - F^x \right] + \frac{\partial}{\partial y} \left[ (S - S^y) \frac{\partial P}{\partial y} - S^{xy} \frac{\partial P}{\partial x} - F^y \right] = 0 \quad (13)$$

where

$$N^x = \frac{Na_{3113}(1 + Na_{3223}) - N^2 a_{3123} a_{3213}}{(1 + Na_{3113})(1 + Na_{3223}) - N^2 a_{3123} a_{3213}}$$

$$N^y = \frac{Na_{3223}(1 + Na_{3113}) - N^2 a_{3123} a_{3213}}{(1 + Na_{3113})(1 + Na_{3223}) - N^2 a_{3123} a_{3213}}$$

$$N^{xy} = \frac{Na_{3123}}{(1 + Na_{3113})(1 + Na_{3223}) - N^2 a_{3123} a_{3213}}$$

$$f^x = \eta N u_{\alpha, \beta a} 31_{\alpha \beta} |_{\alpha \beta} + \int \delta(\tau_{xx, x} + \tau_{yx, y}) d\tilde{z}$$

$$f^y = \eta N u_{\alpha, \beta a} 32_{\alpha \beta} |_{\alpha \beta} + \int \delta(\tau_{zy, z} + \tau_{yy, y}) d\tilde{z}$$

$$S = \int \delta \frac{\tilde{z}^2}{\eta} d\tilde{z} \quad S^x = \int \delta N^x \frac{\tilde{z}^2}{\eta} d\tilde{z}$$

$$S^y = \int \delta N^y \frac{\tilde{z}^2}{\eta} d\tilde{z} \quad S^{xy} = \int \delta N^{xy} \frac{\tilde{z}^2}{\eta} d\tilde{z}$$

$$F^x = \int \delta \frac{\tilde{z}}{\eta} [(1 - N^x) f^x - N^{xy} f^y] d\tilde{z}$$

$$F^y = \int \delta \frac{\tilde{z}}{\eta} [(1 - N^y) f^y - N^{xy} f^x] d\tilde{z}$$

Local Cartesian coordinates are chosen such that  $x$  and  $y$  coordinates are lying on the surface of thin cavity thickness molds,  $z$  being the gap-wise coordinate as shown in Fig. 2.

Boundary conditions on the pressure equation are  $P = 0$  on the moving flow front and  $\bar{u} \cdot \bar{n}_x + v \cdot \bar{n}_y = 0$  on the impermeable boundaries. Pressure equation for fiber suspensions includes the extra terms ( $S_x, S_y, S_{xy}, F_x, F_y$ ) due to the additional stress of fibers, and  $F_x$  and  $F_y$  represent the  $x$  and  $y$  directional in-plane velocity gradient effect. Refer to Chung and Kwon (1995,1996) for the details.

A modified Cross model has been employed for the viscosity of the thermoplastic medium:

$$\eta(\dot{\gamma}, T) = \frac{\eta_0}{1 + (\eta_0 \dot{\gamma} / \tau^*)^m}, \quad \eta_0 = B \exp\left(\frac{T_b}{T}\right) \quad (14)$$

where  $m, B, \tau^*$  and  $T_b$  are constants for a given material.

**energy equation**

$$\rho C_p \left( \frac{\partial T}{\partial t} + u \frac{\partial T}{\partial x} + v \frac{\partial T}{\partial y} \right) = k \frac{\partial^2 T}{\partial z^2} + \eta \dot{\gamma}^2 \quad (15)$$

Appropriate boundary conditions in the  $z$ -direction are the uniform temperature at the mold wall  $z = b$  and the symmetric condition at the mid-plane  $z = 0$

A detailed implementation of numerical analysis is described in Chung and Kwon (1995,1996). In this work, fountain flow and the fiber-wall interaction have been neglected.

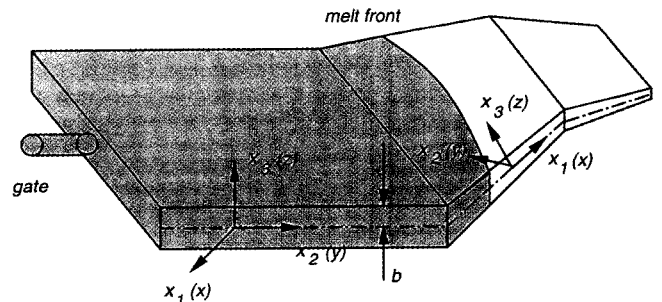


**Fig. 2.** Typical molded part for the analysis. A local coordinate system is chosen so that  $x_3(z)$  is along the thickness direction,  $x_1(x)$  and  $x_2(y)$  lying on the plane.

### 3. Numerical analysis and discussion

We have performed coupled analysis of injection mold filling process including in-plane velocity gradient effects for a film-gated strip and a center-gated disk and compared with experimental measurements of fiber orientation of nylon 6/6 reinforced with 43 wt% ( $v_f = 0.23$ ) of glass fibers (Du Pont: Zytel 101 L)[Bay (1991)]. Non-isothermal, non-Newtonian effects are incorporated. The average fiber length  $L = 210 \mu\text{m}$  and the diameter  $D = 11 \mu\text{m}$ . The thermal properties and melt viscosity constants for the modified Cross model are shown in Table 1. Finite element meshes used for numerical analysis are shown in Fig. 3 and Fig. 4. Cavity geometry data are as follows.

**Film-gated strip:** length  $l = 203.2 \text{ mm}$ , width  $W = 25.4 \text{ mm}$ , and a thickness  $2b = 3.18 \text{ mm}$ .

**Center-gated disk:** outer radius  $R_0 = 76.2 \text{ mm}$  and a thickness  $2b = 3.18 \text{ mm}$ .

$N = 40.3$  is used for simulation based on Dinh and Armstrongs theory with Eqs.9~10. Processing conditions are as follows:

**Film-gated strip:** inlet temperature  $T_{\text{inlet}} = 550 \text{ K}$ , mold wall temperature  $T_{\text{wall}} = 297 \text{ K}$ , and the filling time  $t_{\text{fill}} = 0.4 \text{ s}$ .

**Table 1.** Material properties and viscosity constants of nylon 6/6

Thermal properties (Du Pont: Zytel 70G43L)	
$\rho$	$1.33 \times 10^3 \text{ kg/m}^3$
$C_p$	$1.97 \times 10^3 \text{ J/(kg} \cdot \text{K)}$
$k$	$2.60 \times 10^{-1} \text{ W/(m} \cdot \text{K)}$
Viscosity constants for Cross Model (Du Pont: Zytel 70G43L)	
$m$	0.549
$B$	$4.37 \times 10^{-9} \text{ Pa} \cdot \text{s}$
$T_b$	$1.68 \times 10^4 \text{ K}$
$t^*$	$3.04 \times 10^4 \text{ Pa}$

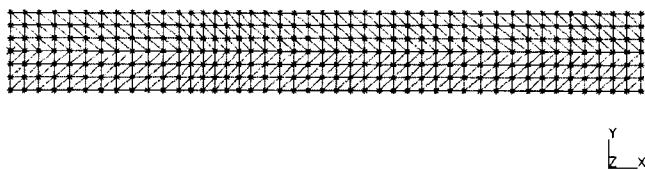


**Fig. 3.** Finite element mesh for rectangular film-gated strip with 528 elements and 315 nodes.

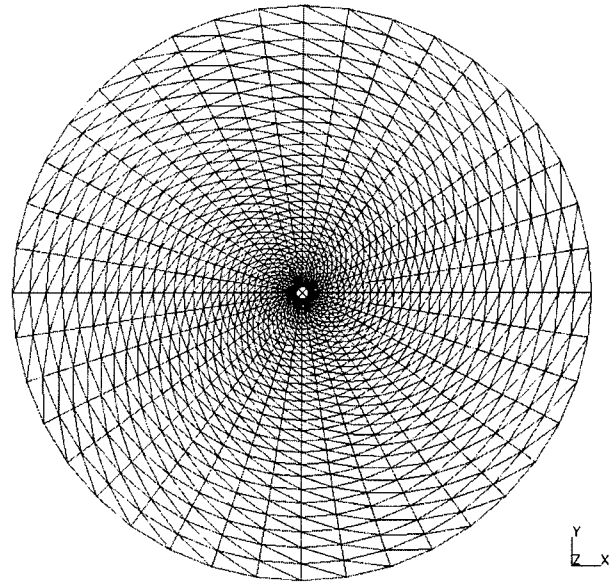


**Fig. 4.** Finite element mesh for a center-gated disk with 2400 elements and 1240 nodes.

**Center-gated disk:**  $T_{\text{inlet}} = 550 \text{ K}$ ,  $T_{\text{wall}} = 347 \text{ K}$ ,  $t_{\text{fill}} = 2.5 \text{ s}$ .

Inlet (initial) orientation state is as follows:

**Film-gated strip:**  $a_{11} = 0.5$ ,  $a_{22} = 0.2$ ,  $a_{33} = 0.3$ ,  $a_{12} = a_{13} = a_{23} = 0$

**Center-gated disk:**  $a_{11} = 1/3$ ,  $a_{22} = 1/3$ ,  $a_{33} = 1/3$ ,  $a_{12} = a_{13} = a_{23} = 0$

Shown in Fig. 5 are flow and thickness directional orientation component ( $a_{11}$  &  $a_{33}$ ) across the thickness at several flow directional locations ( $x/b$ ) for a film-gated strip. To compare results obtained from various closure approximations with experimental data  $C_1 = 0.001$  is used for ORL and other models while  $C_1 = 0.01$  is used for HYB since results from HYB with  $C_1 = 0.001$  is too bad to compare. All of them seem to predict  $a_{11}$  and  $a_{33}$  qualitatively well compared with experimental data. However,  $a_{11}$  shows a little over-prediction of flow directional orientation component at far down-stream, resulting in a thinner core than the experimental data. This point is to be further discussed in conjunction with the center-gated disk case as below.  $a_{33}$  show qualitative agreements with experimental data except the symmetry region ( $z/b = 0$ ) because of no shear deformation.

Shown in Fig. 6 are flow directional orientation component ( $a_{11}$ ) across the thickness at several flow directional locations ( $r/b$ ) for a center-gated disk. In this comparison, the same values of  $C_1$  are used as in the film-gated strip described above. As indicated in Fig. 6, closure models show excellent agreements with experimental data for the range of radial location between the inner radius and about half the radius of the disk. ORW,

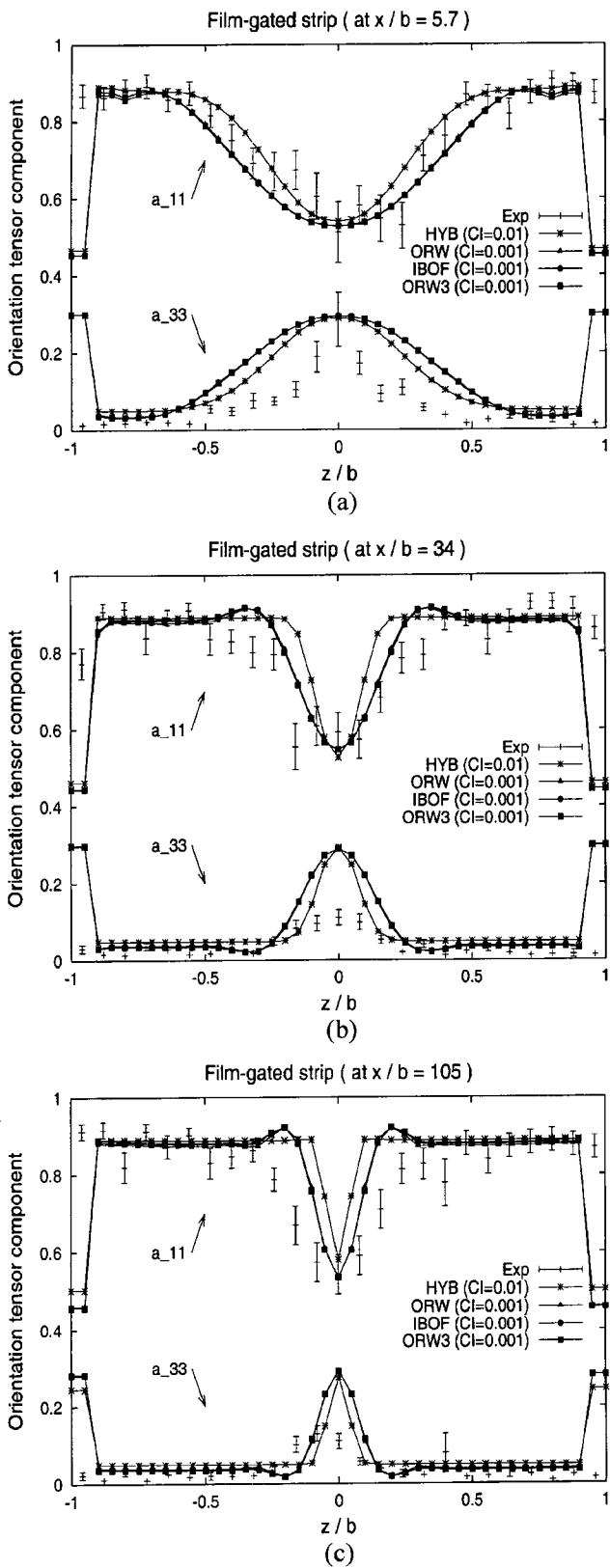


Fig. 5. Orientation component as a function of thickness positions ( $z/b$ ) for various closure approximations of HYB, ORW, IBOF and ORW3 with experimental data for film-gated strip at (a)  $x/b = 5.7$ , (b)  $x/b = 34$ , (c)  $x/b = 105$ .

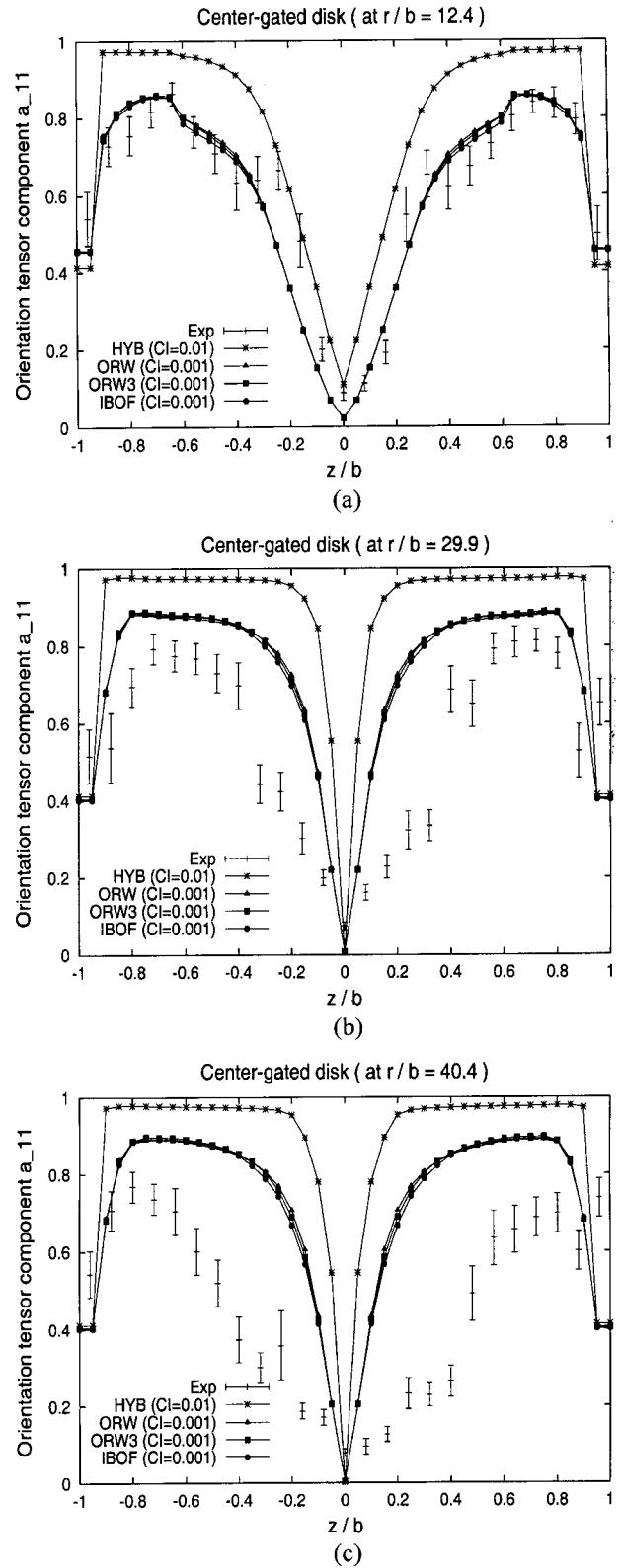


Fig. 6.  $a_{11}$  (flow-directional orientation) component as a function of thickness positions ( $z/b$ ) for various closure approximations of HYB, ORW, ORW3 and IBOF with experimental data for center-gated disk at (a)  $r/b = 12.4$ , (b)  $r/b = 29.9$ , (c)  $r/b = 40.4$ .

ORW3 and IBOF almost show same behaviors.

However, as fiber orientation reaches a steady state, one can observe an over-prediction of flow directional orientation component  $a_{11}$  at core layer (i.e., resulting in too thin core layer) as in the case of the film-gated strip. Assuming that the experimental data are correct, one may consider the following points to account for such a consistent deviation between the numerical prediction and experimental data.

① Compressibility effect by packing stage may affect orientation behaviors, but by intuition, additional velocity components induced by compressibility will further align flow directional orientation component and thus make the core layer thinner. Therefore, considering polymer compressibility effect may not be the right direction to remedy this kind of deviation.

② Diverging effect by thermal boundary layer at wall region (due to conduction from mold wall) induced by a long filling time at center-gated disk may reduce the flow directional orientation component around core layers as a kind of randomization effect. This phenomenon might be observed to some extent around core layer as indicated by the case of  $z/b = 0.2$  in Fig. 7 which shows  $a_{11}$  as a function of radial location ( $r/b$ ) at several thickness positions ( $z/b$ ) in case of IBOF.  $a_{11}$  in the case of  $z/b = 0.2$  starts decreasing around  $r/b = 30$ . This reveals the diverging effect, though not significant, in contrast to  $a_{11}$  at other layers ( $z/b = 0.5, 0.7$ ). However, a strip with a negligible thermal boundary layer due to a short filling time also shows a thin core. So the diverging effect does not make any difference between the film-gated strip

and the center-gated disks despite their different filling time.

③ One may try to modify Folgar and Tucker's model for diffusivity term (more specifically, interaction coefficient  $C_1$  in  $D_r = C_1 \dot{\gamma}$ ), which accounts for the fiber-fiber interaction. According to this model, the orientation is known to reach the steady state rather quickly than the experimental data [Folgar and Tucker (1984)]. It seems natural to conceive that the magnitude of fiber-fiber interaction coefficient may depend on the orientation state especially during the transient and the steady periods. By intuition,  $C_1$  for the transient state must be larger than that of the steady state. This argument has been discussed by many researchers [Folgar and Tucker (1984), Shaqfeh and Fredrickson (1989), Rahnama *et al.* (1994), Stover *et al.* (1992), Fan *et al.* (1998)]. Also, we can verify this argument by performing the coupled simulation of the center-gated disk for  $C_1 = 0.0001$  with ORW3 and IBOF, which are shown in Fig. 8. At far downstream of  $r/b = 40.4$ , predicted orientation component is in much better agreement with experimental data than that for  $C_1 = 0.001$  (Fig. 6). On the other hand, near the gate (at  $r/b = 12.4$ ) the predicted  $a_{11}$  with  $C_1 = 0.001$  is closer to experimental data than that with  $C_1 = 0.0001$ . In summary, it looks plausible that near the gate where orientation state is still transient,  $C_1 = 0.001$  is appropriate and at far downstream where aligned orientation state is reached,  $C_1 \leq 0.0001$  is more appropriate. More study is in order along this line.

#### 4. Concluding Remarks

We have extensively performed numerical analysis of injection molding filling process of fiber suspension in polymer based matrix with recently proposed closure approximations, namely ORW, ORW3 and IBOF. Coupling effect between the fluid flow and the fiber orientation is introduced via Dinh-Armstrong model, along with the in-plane velocity gradient effect in such analyses. Predicted fiber orientations are favorably compared with experimental data for cases of a film-gated strip and a center-gated disk. Simulation results show almost no differences among the fitted closure approximations (ORW, ORW3, IBOF). However, IBOF requires only half the computation time as compared with ORW or ORW3. HYB shows over-prediction of orientation components as expected. Systematic discrepancy between simulation results and experimental data may support, for a better prediction of fiber orientation, to modify the constant isotropic diffusivity term which was used to account for fiber-fiber interaction in the present analyses.

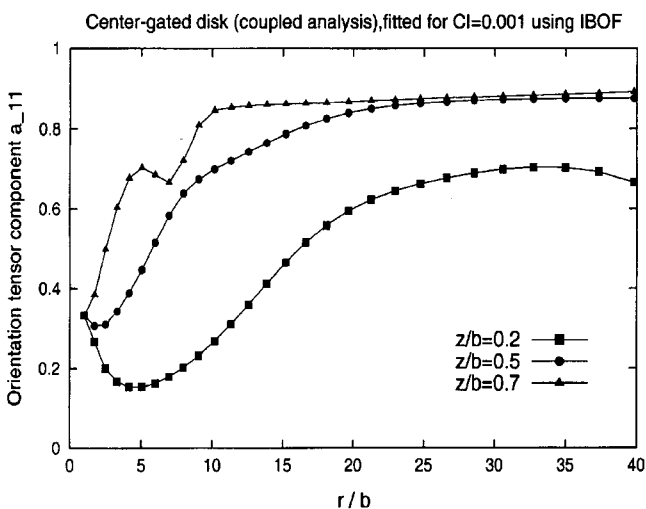


Fig. 7. Plot of  $a_{11}$  (flow-directional orientation) component vs.  $r/b$  for center-gated disk (coupled analysis with in-plane velocity gradient as well as usual shear effect) with  $C_1 = 0.001$  using IBOF closure approximation.

5. List of symbols

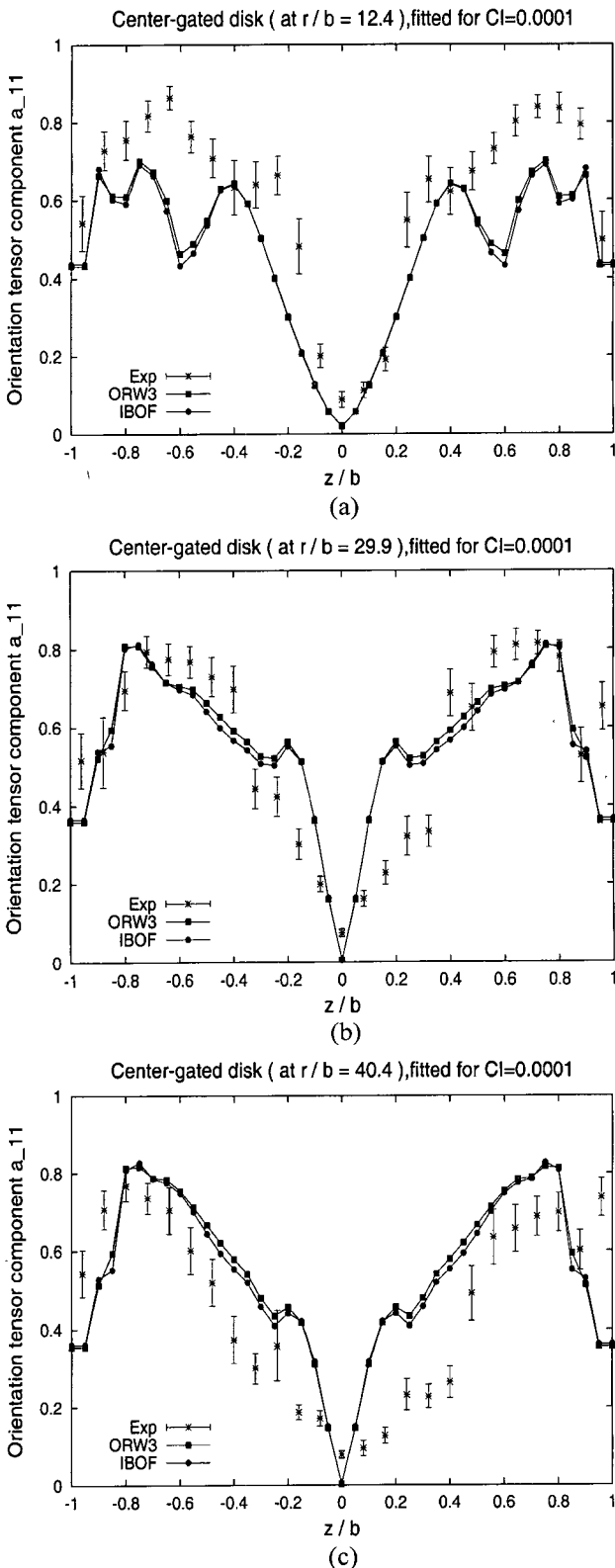


Fig. 8.  $a_{11}$  (flow-directional orientation) component as a function of thickness positions ( $z/b$ ) with  $C_1 = 0.0001$  for closure approximations of ORW3 and IBOF with experimental data for center-gated disk at (a)  $r/b = 12.4$ , (b)  $r/b = 29.9$ , (c)  $r/b = 40.4$ .

- $a_{ij}$  = Second-order orientation tensor.
- $a_{ijkl}$  = Fourth-order orientation tensor.
- $a_{ijkl}^p$  = Fourth-order orientation tensor in reference to eigenspace of second-order orientation tensor (Defined to be principal values of fourth-order orientation tensor in this paper).
- $a_1, a_2, a_3$  = Eigenvalues of second-order orientation tensor in descending order in magnitude.
- $\bar{A}_{mm}$  = Principal values of fourth-order orientation tensor in contracted notation.
- $b$  = Half gap thickness of molded part.
- $C_1$  = Interaction coefficient for fiber-fiber interaction
- $C_p$  = Thermal capacity of the thermoplastic medium.
- $D$  = Fiber diameter.
- $D_r$  = Diffusivity term which accounts for fiber-fiber interaction
- $f$  = Scalar measure of orientation
- $h$  = Average distance from a given fiber to its nearest neighbor.
- $k$  = Thermal conductivity of the thermoplastic medium.
- $l$  = Characteristic length of injection molded part.
- $L$  = Fiber length.
- $n$  = Number of fibers per unit volume.
- $n_x, n_y$  = Components of unit outward normal vector on the boundary.
- $N$  = Dimensionless number accounting for anisotropic contribution from fiber.
- $p$  = Fiber unit direction.
- $p_i$  = Fiber angular velocity.
- $P$  = Pressure.
- $R_0$  = Outer radius of center-gated-disk.
- $t_{fill}$  = Filling time.
- $T$  = Temperature.
- $T_{inlet}$  = Inlet melt temperature.
- $T_{wall}$  = Mold wall temperature.
- $u, v$  = In-plane velocity components with respect to local coordinate.
- $\bar{u}, \bar{v}$  = Gapwise average velocity.
- $u_{i,j}$  =  $\partial u_i / \partial x_j$ , velocity gradient tensor.
- $v_f$  = Volume fraction of fibers.
- $W$  = width of injection molded part.
- $w$  = Gapwise velocity components with respect to local coordinate.
- $x, y, z$  = Local coordinate system.
- $m, B, \tau^*, T_b$  = Coefficients of viscosity function.
- $D/Dt$  = Material derivative.
- I, II, III = First, second and third principal invariants of  $a_{ij}$



### Greek letters

$\Psi$	= Probability distribution function.
$\dot{\gamma}$	= Generalized shear rate.
$\dot{\gamma}_{ij}$	= Rate of deformation tensor.
$\delta_{ij}$	= Unit tensor.
$\eta$	= Viscosity of the thermoplastic medium.
$\eta_0$	= Zero shear rate viscosity.
$\lambda$	= Geometric parameter related to the particle aspect ratio.
$\rho$	= Density of the thermoplastic medium.
$\tau_{ij}$	= Stress tensor.
$\omega_{ij}$	= Vorticity tensor.

### References

- Advani S. G. and C. L. TuckerIII, 1987, The use of tensors to describe and predict fiber orientation in short fiber composites, *J. Rheol.* **31**, 751-784.
- Advani S. G. and C. L. TuckerIII, 1990, Closure approximations for three-dimensional structure tensors, *J. Rheol.* **34**(3), 367-386.
- Batchelor G. K., 1971, The stress generated in a non-dilute suspension of elongated particles by pure straining motion, *J. Fluid Mech.* **46**, 813-829.
- Bay R.S., 1991, Ph.D thesis, Fiber orientation in injection molded composites : A comparison of theory and experiment, University of Illinois at Urbana-Champaign, U.S.A.
- Chung D.H. and T. H. Kwon, 1999, Improved orthotropic closure approximation for fiber orientation tensorial description, in P.G.M. Kruijt, H.E.H. Meijer, F.N. van de Vosse (Eds.), PPS15 Proceedings, Paper 180, Eindhoven University of Technology, Eindhoven.
- Chung D.H. and T.H. Kwon, 2000a, Improved model of orthotropic closure approximation for flow induced fiber orientation, *Polym. Compos.* in print.
- Chung D.H. and T.H. Kwon, 2000b, Invariant based optimal fitting (ibof) closure approximation for numerical prediction of flow induced fiber orientation, *J. Rheol.* submitted.
- Chung S. T. and T. H. Kwon, 1995, Numerical simulation of fiber orientation in injection molding of short-fiber-reinforced thermoplastics, *Polym. Eng. Sci.* **35**, 604-618.
- Chung S. T. and T. H. Kwon, 1996, Coupled analysis of injection molding filling and fiber orientation including in-plane velocity gradient effect, *Polym. Compos.* **17**, 859-872.
- Cintra J. S. and C. L. TuckerIII, 1995, Orthotropic closure approximations for flow-induced fiber orientation, *J. Rheol.* **39**, 1095-1122.
- Dinh S. M. and R. C. Armstrong, 1984, A rheological equation of state for semiconcentrated fiber suspensions, *J. Rheol.* **28**(3), 207-227.
- Dupret F. and V. Verleye, 1999, Modelling the flow of fiber suspensions in narrow gaps, in *Advances in the Flow and Rheology of Non-Newtonian Fluids*, D.A. Siginer, D. De Kee and R.P. Chhabra (Eds.), Rheology Series, 8, Elsevier, Amsterdam, p19-29.
- Fan X.J., N. Phan-Thien and R. Zheng, 1998, A direct numerical simulation of fibre suspensions, *J. Non-Newtonian Fluid Mech.* **74**, 113-135.
- Folgar F. and C. L. TuckerIII, 1984, Orientation behavior of fibers in concentrated suspensions, *J. Reinf. Plast. Compos.* **3**, 98-119.
- Halpin J.C. and J.L. Kardos, 1976, The Halpin-Tsai equations: A review, *Polym. Eng. Sci.* **16**, 344-352.
- Jeffery G. B., 1922, The motion of ellipsoidal particles immersed in a viscous fluid, *Proc. R. Soc.* **A102**, 161-179.
- Lipscomb G. G., M. M. Denn, D. U. Hur and D. Boger, 1988, The flow of fiber suspensions in complex geometries, *J. Non-Newtonian Fluid Mech.* **26**, 297-325.
- Mackaplow M.B. and E.S.G. Shaqfeh, 1996, A numerical study of the rheological properties of suspensions of rigid, non-Brownian fibres, *J. Fluid Mech.* **329**, 155-186.
- Rhanama M., D.L. Koch and E.S.G. Shaqfeh, 1995, The effect of hydrodynamic interactions on the orientation distribution in a fiber suspension subject to simple shear flow, *Phys. Fluids*, **7**(3), 487-506.
- Shaqfeh E.S.G. and G.H. Fredrickson, 1990, The hydrodynamic stress in a suspension of rods, *Phys. Fluids*, **A2**(1), 7-24.
- Stover C.A., D.L. Koch and C. Cohen, 1992, Observations of fibre orientation in simple shear flow of semi-dilute suspensions, *J. Fluid Mech.* **238**, 277-296.
- Sundararajakumar R.R. and D.L. Koch, 1997, Structure and properties of sheared fiber suspensions with mechanical contacts, *J. Non-Newtonian Fluid Mech.* **73**, 205-239.
- Wetzel E.D., 1999, Ph.D thesis, Modeling flow-induced microstructure of inhomogeneous liquid-liquid mixtures, University of Illinois at Urbana-Champaign, U.S.A.
- Verleye, V. and F. Dupret, 1994, Numerical prediction of fiber orientation in complex injection molded parts, Proc. of the ASME Winter Annual Mtg. MD-Vol49. HTD-Vol283, p.264-279.
- Verweyst B.E., 1998, Ph.D thesis, Numerical predictions of flow-induced fiber orientation in three-dimensional geometries, University of Illinois at Urbana-Champaign, U.S.A.
- Yamamoto S. and Matsuoka T., 1993, A method for dynamic simulation of rigid and flexible fibers in a flow field, *J. Chem. Phys.* **98**(1), 644-650.
- Yamane Y., Y. Kaneda and M. Doi, 1994, Numerical simulation of semi-dilute suspensions of rodlike particles in shear flow, *J. Non-Newtonian Fluid Mech.* **54**, 405-421.